Knight shift, spin-lattice relaxation and electric field gradient in technetium metal

2001 J. Phys.: Condens. Matter 13 11041

(http://iopscience.iop.org/0953-8984/13/48/328)

INSTITUTE OF PHYSICS PUBLISHING JOURNAL OF PHYSICS: CONDENSED MATTER

J. Phys.: Condens. Matter **13** (2001) 11041–11051 PII: S0953-8984(01)25106-6

Knight shift, spin–lattice relaxation and electric field gradient in technetium metal

V P Tarasov[1], **Yu B Muravlev**[1] **and K E Guerman**[2]

[1] Institute of General and Inorganic Chemistry, RAS, 117907, Moscow, Russia
[2] UMR 5084, Chimie Nucl. Anal. Bioev., Le Haut Vigneau, BP 120, 33175 Gradignan Cedex, France

E-mail: tarasov@igic.ras.ru

Received 21 November 2000
Published 16 November 2001
Online at stacks.iop.org/JPhysCM/13/11041

Abstract

Spin–lattice relaxation time (T_1), isotropic Knight shift (K_{iso}) and quadrupole coupling constant (C_Q) have been measured in technetium metal by pulsed ^{99}Tc NMR in a magnetic field of 7.04 T in the temperature range 120–400 K. It was found that $(T_1 \times T)^{-1} = 3.21 \pm 0.35$ (s K)$^{-1}$, $K_{iso}(T) = 7305 - 1.52T$ ppm; the quadrupole coupling constant $C_Q = 5.74 \pm 0.05$ MHz is temperature independent. Experimental data on T_1 and K_{iso} are analysed in terms of the contact, d-polarization and orbital hyperfine interactions. It is shown that the main contribution to the relaxation rate comes from the contact interaction and the Knight shift is governed by the orbital interaction. The electric field gradient at the ^{99}Tc nucleus site is considered to be a sum of the electron q^{el} and lattice q^{lat} contributions with different signs. The calculated lattice contribution is positive and constitutes about 30% of the electronic contribution. The obtained values of q^{el} and q^{lat} are compared with data for other metals with hexagonal close-packed lattices.

1. Introduction

Technetium metal crystallizes to form a hexagonal close-packed (hcp) lattice, space group $P6_3/mmm$, $Z = 2$, $a = 2.7407$ Å, $c = 4.398$ Å [1]. Among numerous metals with hcp structure, technetium has the highest superconducting transition temperature ($T_c = 7.8$ K). Technetium is characterized by high catalytic activity and corrosion stability [2]. These practically important properties are responsible for the interest in studying such parameters of the electronic state of technetium metal as the Fermi energy E_F and the density of electron states at the Fermi level $N(E_F)$. For the two most probable electronic configurations of Tc, ($4d^65s^1$) and ($4d^55s^2$), the calculated E_F and $N(E_F)$ are, respectively, 0.67956 Ry, 12.25 states/Ry atom and 0.62998 Ry, 11.87 [3]. Calculations in terms of the cluster model attributed the weak paramagnetic properties of technetium to the presence of unpaired electrons at the

highest occupied level and related the superconducting transition temperature to the density of states at the Fermi level by $T_c \sim N^2(E_F)$ [4].

NMR parameters, such as the Knight shift (K) and its anisotropy (K_{an}), spin–lattice relaxation time (T_1), and the quadrupole coupling constant (QCC), are experimental parameters characterizing the electronic state of a metal with non-cubic lattice. The first study of technetium metal by ^{99}Tc NMR was carried out by Jones and Milford [5]. They determined the isotropic Knight shift $K_{iso} = 7150$ ppm, anisotropy of this shift $K_{an} = 1150$ ppm, linewidth of the central component $\Delta H_{pp} = 13$ Gs and $C_Q = 5.716$ MHz at zero asymmetry parameter of the electric field gradient (EFG) tensor by analysing the lineshape for a Tc powder as a function of resonance frequency (3.2–10.2 MHz). Van Ostenburg *et al* reported $C_Q = 5.05$ MHz, $K_{iso} = 6100$ ppm and a very small anisotropy K_{an} [6, 7]. The spin–lattice relaxation times in technetium metal have been measured at 8 MHz and characterized by the parameter $R = (T_1T)^{-1} = 1.56\,(\mathrm{s\,K})^{-1}$ at 300 K, $1.25\,(\mathrm{s\,K})^{-1}$ at 77.3 K and $1.40\,(\mathrm{s\,K})^{-1}$ at 4.2 K [8]. The obtained R values were entirely attributed to the spin–orbit interaction, in disagreement with the relevant data for other d-metals [9]. In [5–8], measurements were done in rather weak magnetic fields ($B_0 < 1.4$ T) on a wide-line spectrometer with field sweep, which made sufficiently accurate measurement of NMR parameters difficult. Furthermore, nothing was said about the temperature behaviour of the Knight shift and the quadrupole coupling constant. In the present communication we report:

(a) results obtained in studying a polycrystalline sample of technetium metal by ^{99}Tc NMR spectroscopy in a strong field (7.04 T) in the temperature range 120–400 K;
(b) calculated contributions to the magnetic susceptibility, Knight shift and spin–lattice relaxation rate for ^{99}Tc;
(c) calculated lattice and electronic contributions to the electric field gradient in technetium metal.

2. Experimental procedure

A sample of technetium metal for NMR measurements was prepared by reduction of tetramethylammonium pertechnetate $(CH_3)_4NTcO_4$ (99.99% purity) in a gas mixture (94% H_2 + 6% Ar) at 1150 K. The sample was cooled to room temperature, crushed in an agate mortar and then a fraction with 80–150 μm dispersity was separated and placed in a 30 mm long Teflon ampoule with outer diameter of 10 mm. According to mass-spectrometric data, the total concentration of the basic impurities Ni, Fe, Al did not exceed 3×10^{-3}%. The weight of the technetium metal sample was 1.16 g. To prevent intergranular contacts, the powder was embedded in an Apiezon/dodecane suspension (1:20) (with drying at room temperature).

^{99}Tc NMR measurements were done on a Bruker MSL-300 spectrometer in a magnetic field of 7.04 T at a frequency of 67.55 MHz in the temperature range 120–400 K. The sample temperature was controlled using a B-VT-1000 unit. To record spectra in a 2.5 MHz spectral window, the spin system was excited by short 0.6 μs pulses with repetition time of 0.5 s and reciever dead time of 5 μs. A total of 50 000 free-induction decays were accumulated. The obtained free-induction signal was multiplied by a smoothing function with subsequent Fourier transformation. Some spectra were recorded using two-pulse spin-echo sequence $\{\theta_x - \tau - \theta_y - ACQ\}$ with selection pulse width ($\theta = 3.22$ μs) calculated from the expression $\theta = \theta(90)/I + 1$, where $I = 9/2$, and $\theta(90) = 16.1$ μs is a 90° pulse measured for the peak ^{99}Tc NMR signal in an aqueous solution of $KTcO_4$ (0.1M). The position of the signal in this solution was taken as reference point for calculating ^{99}Tc NMR shifts in technetium metal.

Spin–lattice relaxation times were measured for the signal of the central component

$(1/2 \Leftrightarrow 1/2$ transition) at a scan width precluding observation of satellites, using the standard saturation-recovery technique $\{\theta_x - \tau - \theta_y\}_n - \tau - \theta_y$, with $\theta = 3.22\,\mu$s, $\tau_1 = 10\,\mu$s and $n = 80$, optimized for the minimum signal. The time delay was varied between 50 μs and 10 ms, and the number of delays, between 14 and 17.

3. Experimental results

The ^{99}Tc NMR line (spin $I = 9/2$) for a polycrystalline sample of technetium metal at 297 K (figure 1(a)) comprises $2I = 9$ lines, including the central line and four symmetrically located pairs of satellites due to first-order quadrupole interactions. These eight satellites correspond to the transitions $(\pm 9/2 \Leftrightarrow \pm 7/2)$, $(\pm 7/2 \Leftrightarrow \pm 5/2)$, $(\pm 5/2 \Leftrightarrow \pm 3/2)$, $(\pm 3/2 \Leftrightarrow \pm 1/2)$. With allowance made for line broadening resulting from powder averaging, the intensity of satellites in the experimental spectrum agrees with the theoretical ratio of integrated intensities for the 9/2 spin: 9:16:21:24:25:24:21:16:9 [10]. The theoretical spectrum for $I = 9/2$ is shown in figure 1(b) in the form of a histogram. The observed lineshape of the satellites corresponds to a zero asymmetry parameter of the EFG tensor, $\eta = 0$. The splitting in kilohertz measured between the closest-spaced pair of satellites, is the lowest frequency of the quadrupole transition $\nu_Q = 239.1$ kHz, which corresponds to the quadrupole coupling constant for $I = 9/2$

$$C_Q = \frac{e^2 q Q}{h} = \frac{2}{3} I(2I-1)\nu_Q = 24\nu_Q = 5.74\,\text{MHz}.$$

In the whole investigated temperature range, the lineshape of the satellites and the ν_Q values remain unchanged. The temperature dependence of the quadrupole transition frequency is shown in figure 2(a).

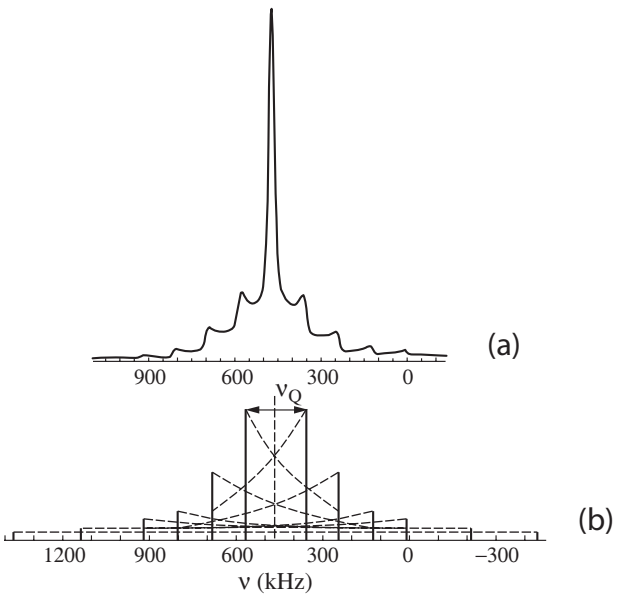

Figure 1. ^{99}Tc NMR lineshape in polycrystalline sample of technetium metal at 297 K in a field $B_0 = 7.04$ T. (a) single-pulse sequence (pulse width 0.6 s, spectral width 2.5 MHz, repetition time 100 ms, receiver dead time 5.4 μs, number of scans 50 000). (b) histogram of satellite distribution in the NMR spectrum for spin $I = 9/2$ and zero asymmetry parameter of the EFG tensor.

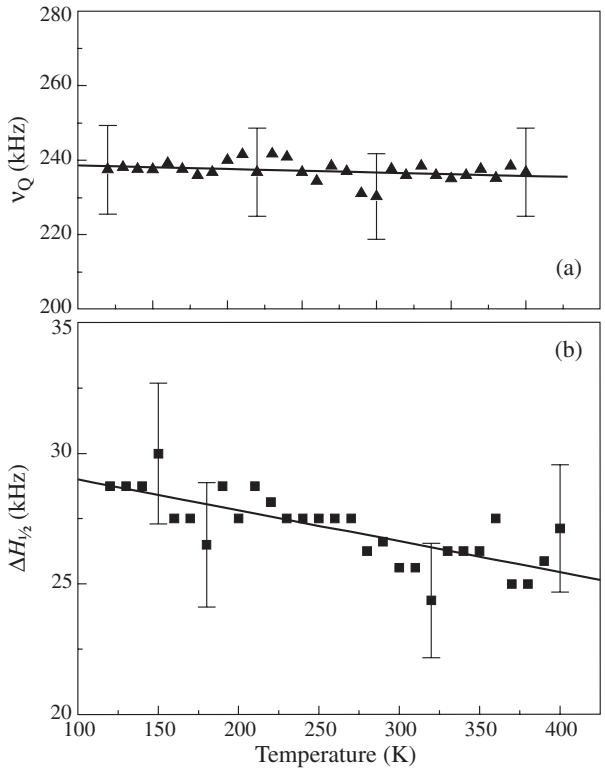

Figure 2. Temperature dependences of (*a*) quadrupole transition frequency ν_Q (measured between the closest-spaced pair of satellites) and (*b*) full width at half-maximum of the central component in the spectrum of technetium metal.

The central component is symmetric with a full width at half-maximum $\Delta\nu_{1/2} = 27.5 \pm 1.0$ kHz at 297 K and the distance measured between the peaks of the absorption derivative $\Delta\nu_{pp} = 15.8 \pm 0.5$ kHz. The ratio $\Delta\nu_{1/2}/\Delta\nu_{pp} = 1.74$ corresponds to a Lorentzian lineshape [11]. A simulation of the central component by the LineSim program[1] also gives a Lorentzian contour with $\Delta\nu_{pp} = 15.5$ kHz. The temperature dependence of $\Delta\nu_{1/2}$ is weak (figure 2(*b*)), being described by an empirical linear relation $\Delta\nu_{1/2} = 28.2 - 0.01T$ (kHz) in the range 120–400 K.

The basic reasons for line broadening in metals are as follows [9]:

(a) static direct dipole–dipole interaction of nuclear spins,
(b) scalar and pseudo-dipole interactions,
(c) electric quadrupole interaction (for metals with non-cubic lattice),
(d) anisotropy of the Knight shift, manifesting itself in inhomogeneous line broadening.

Since technetium-99 is a 100% artificial isotope, the scalar interaction between identical spins does not contribute to the linewidth, and the contribution from the pseudo-dipole interaction is rather small. The contribution from the second-order quadrupole interaction to the broadening of the central component can be calculated exactly. Since the ratio of the lowest quadrupole frequency ν_Q to the Larmor frequency ν_L is $\nu_Q/\nu_L = 230 \times 10^3/67.55 \times 10^6 =$

[1] Included in the Aspect-3000 software.

$0.003 \ll 1$, the splitting of the central component $\nu_Q^{(2)}$ through second-order quadrupole interactions is $\nu_Q^{(2)} = 25\nu_Q^2/6\nu_L = 3.26$ kHz at $\eta = 0$. Such a small splitting, compared to the linewidth of 25 kHz, is not observed in experiment as asymmetry of either the absorption line or its first derivative. Thus, there only remain two sources of broadening: (i) direct dipole–dipole interaction, and (ii) Knight shift anisotropy. The first of these can be estimated from the second moment of the central component [10]

$$\langle \nu^2 \rangle = \frac{1}{4}\pi^2 F(I)\gamma^4 h^2 \sum_k b_{jk}^2 \quad \text{kHz}^2$$

where $F(I)$ is a complicated function of the nuclear spin $F(I) = 4/27I(I+1) + \{2I^2)(I+1)^2 + 3I(I+1) + 13/8\}/18(2I+1) = 1961/180$ at $I = 9/2$.

$$\langle b^2 \rangle = \frac{9}{5}\sum_k r_{kj}^{-6} \qquad \langle \nu^2 \rangle = 7.25 \times 10^{-40} \sum_k r_{jk}^{-6}$$

where r_{jk} is the distance between jth and kth technetium nuclei in the lattice. For the ideal hcp lattice the ratio between the height c of the unit cell and its base edge a is $c/a = \sqrt{8/3} = 1.639$. Only at this ratio all the nearest 12 atoms are at the same distance from a chosen technetium atom. For a actual hcp lattice of technetium, $c/a = 1.6047$. Therefore, the nearest 12 atoms are divided into 6 atoms in a horizontal sheet at a distance $r_1 = a = 2.7407$ Å and 3 + 3 atoms below and above this sheet at $r_2 = \sqrt{a^2/3 + c^2/4} = 2.709$ Å. Then, the lattice sum $\sum_k r_{kj}^{-6}$ within a single unit cell radius is $29.2 \times 10^{45}\,\text{cm}^{-6}$, and the second moment $\langle \nu^2 \rangle = 21.2\ \text{kHz}^2$. The Lorentz linewidth at this second moment value is estimated to be $\langle \Delta\nu \rangle = \sqrt{(\pi\langle \nu^2 \rangle/2)} = 5.8$ kHz, which is ~5 times less than the experimental value. Thus, it only remains to accept that the observed linewidth is determined by the Knight shift anisotropy $(K_\perp - K_\parallel) = -400$ ppm. The sign of this anisotropy was determined by comparing the positions of the central line K and the K_{iso} value calculated from the position of the satellite centre $K_{iso} - K = 20$ ppm. At a ratio between the Lorentzian linewidth $\Delta\nu_{1/2}$ and the shift anisotropy equal to 0.2–0.3, the resulting line is broadened and its envelope becomes practically symmetric with a downfield-shifted peak [11].

The temperature dependence of the Knight shift K, measured as the position of the central component, can be described by the following linear relation: $K = 7305 - 1.52T$. K changes with temperature change by ~8% (figure 3(*a*)).

The spin–lattice relaxation time $T_1(^{99}\text{Tc})$ was measured for the central spectral component by the saturation-recovery technique. The dependence of the peak amplitude (and the integrated intensity) of an NMR signal on the delay time τ is described by a one-exponent function. With account taken of the measurement errors (11%), the experimental data on T_1^{-1} as a function of temperature can be approximated by $T_1^{-1} = 231(30) + 2.2(1)T\ \text{s}^{-1}$. Such a behaviour reveals both the temperature-independent contribution and the term linear in temperature, expected for metals. Over the entire temperature range, $(T_1 \times T)$ slightly changes and/or has a scatter between 0.24 and 0.36 s K with average value 0.31 ± 0.05 s K. This value was used in further estimation of contributions. This result shows that the dominant mechanism of spin–lattice relaxation is the interaction of ^{99}Tc spins with conduction-band electrons. At $K = 7 \times 10^{-3}$ the experimental value $(K^2T_1T) = 15.2 \times 10^{-6}$ s K, which is ~3 times greater than $(K_s^2T_{1s}T)$ for the s-contact interaction calculated using the Korringa relation: $(K_s^2T_{1s}T) = \hbar/4\pi k_B(\gamma_e/\gamma_{Tc})^2 = 5.2 \times 10^{-6}\,\text{K}^{-1}\,\text{s}^{-1}$, where $(\gamma_e/\gamma_{Tc})^2 = 0.085 \times 10^8$, k_B is the Boltzmann constant. Korringa's theoretical expression is valid in the approximation of non-interacting electrons. Therefore, to analyse experimental data, account should be taken of

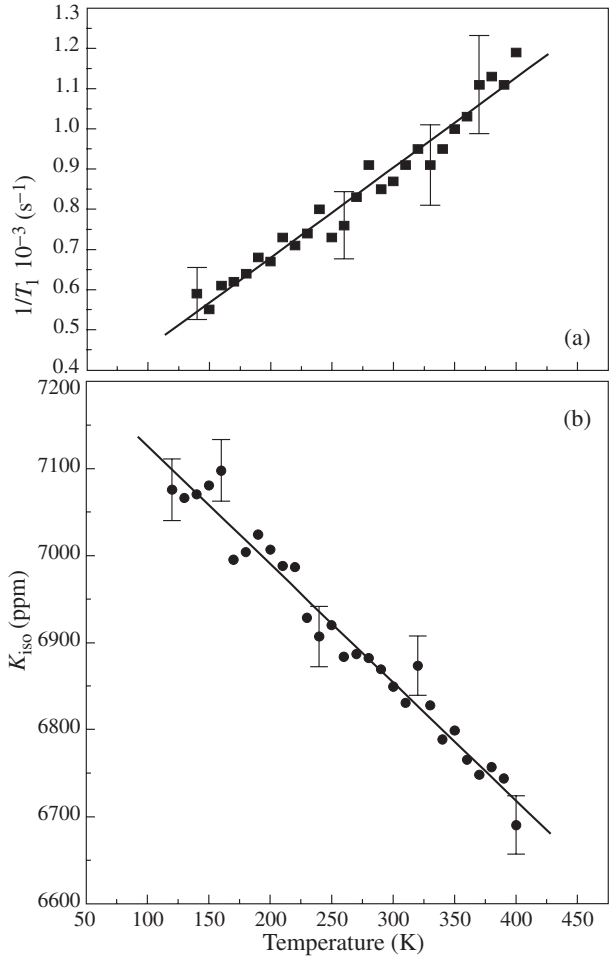

Figure 3. Temperature dependences of (*a*) spin–lattice relaxation rate (T_1^{-1}) and (*b*) isotropic Knight shift K_{iso} for technetium metal.

both electron–electron interactions and contributions to the Knight shift and the spin–lattice relaxation rate not only from the s-contact interaction but also from other possible hyperfine interactions due to d-electrons.

4. Discussion

For 4d-metals, the Knight shift (K), spin–lattice relaxation time (T_1) and magnetic susceptibility (χ) are analysed in terms of the two-band (s- and d-) model and the model of additive contributions associated with [9]:

(a) contact interaction with conduction-band s-electrons (s-contribution);
(b) contact interaction with closed-shell s-electrons due to their polarization by conduction-band d-electrons (polarization d-contribution);
(c) orbital interaction with d-electrons from partially filled shell (orbital contribution);
(d) spin–dipole interaction for non-cubic metals (dipole contribution).

The relative contributions depend on the electronic structure of a metal. Let us consider how the above interactions affect the spin–lattice relaxation rate and the Knight shift in technetium metal.

4.1. Spin–lattice relaxation

A theory of spin–lattice relaxation in transition metals, accounting for electron–electron interactions, has been developed by Yaffet and Jaccarino [12] for the cubic lattice and by Narath [13] for the hcp structure in terms of additive contributions:

$$R = R_{\mathrm{s}} + R_{\mathrm{cp}} + R_{\mathrm{orb}} + R_{\mathrm{d}}. \tag{1}$$

For ^{99}Tc spins we can write the expressions $R_i = (T_{1i} \times T)^{-1}$ for each contribution in $(\mathrm{s\,K})^{-1}$ units as follows:

$$R_{\mathrm{s}} = (T_{1\mathrm{s}}T)^{-1} = \frac{4\pi}{h}\left[\gamma_n h H_{\mathrm{s}} N_{\mathrm{s}}\right]^2 = 66.28 \times 10^{-36}\,[H_{\mathrm{s}}N_{\mathrm{s}}]^2 = 407.6 \times 10^{-24} N_{\mathrm{s}}^2 \tag{2}$$

$$\begin{aligned} R_{\mathrm{cp}} = (T_{1\mathrm{cp}}T)^{-1} &= \frac{4\pi}{h}\left[\gamma_n h H_{\mathrm{d}} N_{\mathrm{d}}\right]^2 q = 66.28 \times 10^{-36}\,[H_{\mathrm{d}}N_{\mathrm{s}}]^2\, q(f) \\ &= 2.92 \times 10^{-24} N_{\mathrm{d}}^2 q(f) \end{aligned} \tag{3}$$

$$\begin{aligned} R_{\mathrm{orb}} = (T_{1\mathrm{orb}}T)^{-1} &= \frac{4\pi}{h}\left[\gamma_n h H_{\mathrm{orb}} N_{\mathrm{d}}\right]^2 p = 66.28 \times 10^{-36}\,[H_{\mathrm{orb}}N_{\mathrm{d}}]^2\, p(f) \\ &= 5.38 \times 10^{-24} N_{\mathrm{d}}^2 p(f) \end{aligned} \tag{4}$$

$$R_{\mathrm{dip}} = (T_{1\mathrm{dip}}T)^{-1} = \tfrac{1}{25} R_{\mathrm{orb}} \tag{5}$$

where $\gamma_n(^{99}\mathrm{Tc})/2\pi = 958.3\,\mathrm{Hz\,G^{-1}}$; H_{s}, H_{d}, H_{orb} are hyperfine magnetic fields per electron (in oersteds) determining the contact, polarization and orbital contributions, respectively, to interactions with ^{99}Tc nucleus spin; N_{s} and N_{d} are the densities of s- and d-states at the Fermi level for a single spin orientation. As a result of electron–electron Coulomb interactions, the functions $q(f)$ and $p(f)$ describe the admixture of $4\mathrm{d}(\Gamma_5)$ states at the Fermi surface[2] [13]. The numerical values of hyperfine fields at an atom and in technetium metal are listed in table 1. The total density of states at the Fermi surface, $N(E_{\mathrm{F}})$, is calculated using the Sommerfeld expression $N(E_{\mathrm{F}}) = 3c_{\mathrm{e}}/T2\pi^2k_{\mathrm{B}}^2 = 7.5 \times 10^{11}$ emu/atom, where the electronic specific heat of technetium $c_{\mathrm{e}}/T = 5.61\,\mathrm{mJ\,mol^{-1}\,K^{-2}}$ [14][3]. Assuming $N_{\mathrm{s}}/N = 0.1$ and $N = N_{\mathrm{s}} + N_{\mathrm{d}}$, we find $N_{\mathrm{s}} = 0.75 \times 10^{11}$ emu/atom and $N_{\mathrm{d}} = 6.75 \times 10^{11}$ emu/atom. With account of these data, contributions to the spin–lattice relaxation were calculated for two values $f = 1$ and $f = 0.6$, using expressions (2)–(5) (see table 1). The dipole contribution determined from formula (5) is $R_{\mathrm{dip}} = 0.02{-}0.04\ (\mathrm{s\,K})^{-1}$ and can be neglected. As it can be seen from table 1, the total calculated contribution is in good agreement with the experimental value. Comparison of the calculated contributions indicates that technetium has the greatest relaxation contribution associated with the contact interaction, similarly to molybdenum, but unlike vanadium, niobium [12] and palladium [9].

[2] For the hcp lattice, the expressions for R_{cp} and R_{orb} include two parametric functions $q(x, y)$ and $p(x, y)$ characterizing the anisotropy of relaxation of these contributions. At $x = 0.8$ and $y = 0.5$, the anisotropy vanishes and these functions become one-parameter functions, $q(f)$ and $p(f)$, having the same form as those for the cubic lattice, $q(f) = 1/3f^2 + 1/2(1-f)^2$ and $p(f) = 2/3f[2 - 5/3f]$ [13]. To evaluate R_{cp} and R_{orb}, we used two f values, 1 and 0.6, at which $q = 0.33$ and 0.2, $p = 0.2$ and 0.4, respectively.

[3] Of the following three values of electronic specific heat c_{e}/T for technetium metal: 4.3, 5.61 and $6.28\,\mathrm{mJ\,mol^{-1}\,K^{-2}}$, the second (5.61) was chosen.

Table 1. Hyperfine fields for 5s, 4d electrons of technetium in atomic state and in metal, contributions to the rate of spin–lattice relaxation and the Knight shift.

Interactions	H_{hf} 10^{-6} (Oe)		R (s K)$^{-1}$		K (ppm)
	atom	metal[a]	$f = 1$	$f = 0.6$	
Contact	3.55[b]	2.48	2.29	2.29	3462
d-polarization	−0.21[c]	−0.21	0.44	0.27	−2631
Orbital	0.40[b]	0.28	0.49	0.98	6031
Total					
calculated			3.23	3.54	
experiment			3.21±0.35		

[a] The ratios between hyperfine fields in metal and atom are [9,12]: $\chi_s = H(s)_m/H(s)_a = 0.7$; $\chi_d = H(d)_m/H(d)_a = 1.0$; $\chi_{orb} = H(d)_m/H(d)_a = 0.75$.
[b] From [12]
[c] Obtained from analysis of the hyperfine structures of ESR spectra of Tc^{+4} in a $KPtCl_6$ single-crystal at 4.2 K, $K_{hf} = 148$ G [15].

5. Knight shift and magnetic susceptibility

Similarly to the case of spin–lattice relaxation, three types of interactions give rise to the Knight shift, with only K_{cp} taken to be temperature dependent [16]:

$$K(T) = K_s + K_{cp}(T) + K_{orb}. \tag{6}$$

For any kind of interaction, the Knight shift is related to the respective hyperfine field H_{hf} and magnetic susceptibility :

$$K^{(i)} = (\mu_B A)^{-1} H_{hf}^{(i)} \chi^{(i)} = 1.79 \times 10^{-4} H_{hf}^{(i)} \chi^{(i)} \tag{7}$$

where μ_B is the Bohr magneton and A is Avogadro's number. The expressions for separate contributions to the Knight shift are as follows:

$$K_s = 1.79 \times 10^{-4} H_s \chi_s \tag{8}$$

$$K_{cp}(T) = 1.79 \times 10^{-4} H_d \chi_d(T) \tag{9}$$

$$K_{orb} = 1.79 \times 10^{-4} H_{orb} \chi_{vv} \tag{10}$$

χ_s and χ_d are calculated using the densities of states N_s and N_d $\chi_s = 2\mu_B^2 N_s A = 7.8 \times 10^{-6}$ emu mol^{-1}, $\chi_d = 2\mu_B^2 N_d A = 70 \times 10^{-6}$ emu mol^{-1}.

Then, the resulting shifts take the following values $K_s = 3462$ ppm, $K_{cp} = -2631$ ppm.

Since the orbital susceptibility χ_{vv} is unknown, we determined the orbital contribution K_{orb} from the differences between the experimental K and calculated contributions K_s and K_{cp}: $K_{orb} = K - K_s - K_{cp} = 6031$ ppm. Using this orbital contribution and the hyperfine orbital field H_{orb}, we obtained the orbital susceptibility $\chi_{vv} = 120 \times 10^{-6}$ emu mol^{-1}. The total susceptibility due to electron conduction $\chi_{calc} = 2/3\chi_s + \chi_d + \chi_{vv} = 195.2 \times 10^{-6}$ emu mol^{-1}. With account of the assumptions made, this value is in rather good agreement with the experimental value of 270×10^{-6} emu/atom [17]. It should be noted that the measured values χ are somewhat temperature dependent, varying from 250×10^{-6} emu/atom at 402 K to 270×10^{-6} emu/atom at 298 K and 290×10^{-6} emu/atom at 78 K [17], which is about 14% of the total susceptibility. The temperature variation of the Knight shift in the temperature range 120–400 K is ∼400 ppm, which also equals ∼14% of the temperature dependent contribution $K_{cp}(T) = -2631$ ppm. For the known thermal expansion coefficients of technetium metal, $\alpha_a = 7.04 \times 10^{-6}$ K^{-1} and $\alpha_c = 7.06 \times 10^{-6}$ K^{-1} [1], the change in the unit cell volume in the range 100–400 K does not exceed 0.6%, which presumably rules out any contribution of the volume effects to the observed temperature dependences $\chi(T)$ and $K(T)$.

Now, knowing the Knight shift and relaxation rate for each type of hyperfine interactions, we can calculate using the Korringa relation:

$$\left(K_s^2 T_{1s} \times T\right)_{calc} = (3.462 \times 10^{-3})^2 \times 0.44 = 5.27 \times 10^{-6}\,\mathrm{s\,K}$$

$$\left(K_{cp}^2 T_{1cp} \times T\right)_{calc} = (2.631 \times 10^{-3})^2 \times 2.2 = 15.23 \times 10^{-6}\,\mathrm{s\,K}.$$

The first value is in good agreement with the theoretical Korringa constant, and the second, with the experimental value. The numerical agreement between $(K_s^2 T_1\, T)$ and the theoretical Korrinda constant points to the correctness of the K_s and T_{1s} estimates. Since $K_{cp}(T)$ and $\chi(T)$ exhibit a noticeable temperature dependence, this result can be attributed, according to [9], to electron–electron interactions. For the orbital contribution, the Korringa relation is not obeyed, since the shift is determined by all d-electrons, and the relaxation, only by d-electrons located at the Fermi level.

6. Electric field gradient

The electric field gradient (EFG) q is related to the quadrupole coupling constant C_Q by

$$q^{exp}[\mathrm{cm}^{-3}] = 2.873 \times 10^{22} \frac{C_Q\,(\mathrm{MHz})}{Q\,(\mathrm{b})} \tag{11}$$

where Q is the quadrupole nucleus momentum. For $Q(^{99}\mathrm{Tc}) = 0.3$ b and $C_Q = 5.74$ MHz, the EFG magnitude at a Tc site is $q^{exp}(^{99}\mathrm{Tc}) = 55.0 \times 10^{22}\,\mathrm{cm}^{-3}$.

For metals with non-cubic lattice, q at nuclear sites is commonly represented as a sum of the lattice contribution q^{lat}, multiplied by the Sternheimer factor $(1 - \gamma_\infty)$, and the electronic contribution q^{el} due to conduction electrons of types other than the s-type: $q = (1 - \gamma_\infty)q^{lat} + q^{el}$. We estimated the lattice contribution to the EFG of ^{99}Tc within the framework of de Wette's theory for an hcp lattice [18] at $c/a = 1.604$ and $a = 2.7407$ Å:

$$Z^{-1}q^{lat} = 0.66 \times 10^{22}\,\mathrm{cm}^{-3} \tag{12}$$

where Z is the effective nuclear charge. Assuming Z equal to the number of valence electrons, $Z(\mathrm{Tc}) = 7$, we get an estimate of the lattice contribution to the technetium EFG: $(1 - \gamma_\infty)q^{lat} = +27.0 \times 10^{22}\,\mathrm{cm}^{-3}$ for $\gamma_\infty(\mathrm{Tc}) = -5$ [19]. To be sure, the effective charge Z(Tc) is lower than the formal value 7 because of the localized character of 4d-electrons, and the obtained lattice contribution is obviously overestimated. Therefore, it is helpful to compare the lattice and electronic contributions to EFG for other metals with the hcp lattice. These data are listed in table 2. According to de Wette's theory [18], the lattice contribution $a^3 Z^{-1} q^{lat}$ is determined by the parameter a of the hcp lattice and the c/a ratio. At around $c/a = 1.6345$, the lattice contribution changes its sign to become negative at greater c/a, as, e.g., in zinc. For the other metals listed in table 2, this contribution is positive. The $Z^{-1}q^{lat}$ calculated for the known hcp lattice parameters of the metals considered are given in the fifth column. In calculating the lattice contribution $(1-\gamma_\infty)q^{lat}$, we assumed the effective charge Z to be equal to the number of valence electrons in the corresponding element: 3 for Sc and La, 4 for Ti, 7 for Tc, Re, 8 for Ru and 2 for Zn. The Sternheimer antishielding factor $(1 - \gamma_\infty)$ was taken to be 8 for scandium and titanium [13], 69 for lanthanum [21], 28.3 for rhenium and 13.7 for zinc [26]. Assuming that the lattice and electron contributions have different signs, as is the case for beryllium [26] and lanthanum [20], we calculated the electronic contribution to EFG (on the condition that $|q^{el}| > |q^{lat}|$). The obtained q^{el} values are given in the last column of table 2. Because of the uncertainty in Z, quadrupole moments Q and antishielding factors $(1 - \gamma_\infty)$, these values are only estimates. It should be noted that the lattice contribution does

Table 2. Quadrupole coupling constants and total, electron and lattice contributions to EFG for metals with hcp lattice.

Metal isotope	C_Q[a] MHz	$\lvert q^{exp}\rvert$[b] 10^{-22} cm^{-3}	c/a for hcp lattice	$Z^{-1}q^{lat}$ 10^{-22} cm^{-3}	$(1-\gamma_\infty)q^{lat}$ 10^{-22} cm^{-3}	q^{el} 10^{-22} cm^{-3}
^{45}Sc	2.02 [20]	26.12	1.5936	0.498	12	−34.12
^{139}La	1.41 [20]	19.3	1.6125	0.183	38.3	−57.6
^{47}Ti	10.8 [21]	107.0	1.601	0.85	27.2	−134.2
^{49}Ti	8.3 [21]	99.4	1.601	0.85	27.2	−126.6
^{99}Ru	0.843 [22]	31.9	1.5808	1.19	—	—
^{101}Ru	5.0 [22]	32.6	1.5808	1.19	—	—
^{99}Tc	5.74[c]	55.0	1.6047	0.642	27.0	−82
^{187}Re	274 [23]	302.8	1.6196	0.31	61.4	−241.4
^{67}Zn	12.73 [24]	243.8	1.8563	−5.17	−141.7	102.1

[a] Measured at room temperature; for ruthenium and zinc at 4.2 K
[b] Calculated using expression (11) for the following values of quadrupole moments in barns [23]: $Q(^{45}\text{Sc}) = -0.22$; $Q(^{139}\text{La}) = 0.2$; $Q(^{47}\text{Ti}) = 0.29$; $Q(^{49}\text{Ti}) = 0.24$; $Q(^{99}\text{Ru}) = 0.076$; $Q(^{101}\text{Ru}) = 0.44$; $Q(^{99}\text{Tc}) = 0.3$; $Q(^{187}\text{Re}) = 2.6$; $Q(^{67}\text{Zn}) = 0.15$.
[c] From this work.

not exceed 50% of the electronic contribution in all the transition metals, but predominates in zinc.

It is commonly believed that the temperature dependence of EFG in pure metals obeys the equation [26]: $q(T) = q(0)[1 - \beta T^{3/2}]$, $\beta > 0$. Theoretical substantiation of this equation is related to temperature-induced changes in root-mean-square displacements of atoms or in the phonon spectrum of the lattice. However, as follows from the experiment (figure 2(*a*)), the EFG in technetium metal is temperature independent in the temperature range studied to within the experimental error. The reasons for such behaviour are unclear. One of the possible explanations of why the EFG is temperature independent is based on an assumption that the absolute values of both q^{el} and q^{lat} contributions undergo identical changes with temperature, but, because of the opposite signs of the lattice and electronic contributions, these changes cancel out, with the total EFG remaining constant. This assumption needs theoretical substantiation.

7. Conclusion

Experimental data on the temperature dependences of the Knight shift, spin–lattice relaxation rate and quadrupole coupling constant in technetium metal are presented. These parameters and the magnetic susceptibility are consistently interpreted in terms of the hyperfine contact, polarization and orbital interactions. The major contribution to the Knight shift comes from the orbital interaction. The temperature dependence of the Knight shift is determined by the polarization contribution whose value reflects the electron–electron Coulomb interaction. The contact interaction is the most efficient channel determining the relaxation rate. The quadrupole coupling constant remains temperature independent over the whole temperature range studied. The estimated lattice contribution to EFG is 30%, which is common to transition metals. We believe that the obtained experimental data and the calculated contributions for a bulk sample will be helpful in making a comparison with the relevant NMR parameters for nanosize particles of technetium metal.

Acknowledgments

The authors are grateful to Professor A A Vashman for critical coments and helpful discussions of this work.

References

[1] Rard J A, Rard M H, Anderegy G, Wanner H 1999 *Chemical Termodynamic of Technetium* ed M C A Sandino and E Osthols, OECD NEA, Data Bank, Issy-les-Moulineaux, France
[2] Spitsin V I and Kuzina A F 1981 *Technetium* (Moscow: Nauka)
[3] Faulkner J S 1977 *Phys. Rev.* B **16** 736
[4] Plechanov Yu V 1999 *The second Japan-Russian Seminar on Technetium* Abstracts, Shizuoka, Japan, p 13
[5] Jones W H and Milford F J 1962 *Phys. Rev.* **125** 1259
[6] Van Ostenburg D O, Trapp H and Lam D J 1962 *Phys. Rev.* **126** 938
[7] Van Ostenburg D O, Lam D J, Trapp H and Mac Lead D E 1962 *Phys. Rev.* **128** 1550
[8] Van Ostenburg D O, Sporas J J and Lam D J 1965 *Phys. Rev.* A **139** 713
[9] Winter J 1971 *Magnetic Resonance in Metals* (Oxford: Clarendon Press)
[10] Abragam A 1961 *The Principles of Nuclear Magnetism* (Oxford: Clarendon Press)
[11] Pool C P 1967 *Electron Spin Resonance* (N-Y, London, Sydney: Willey)
[12] Yafet Y and Jaccarino V 1964 *Phys. Rev.* A **133** 1630
[13] Narath A 1967 *Phys. Rev.* **162** 320
[14] Roberts B W 1976 *J Phys. Chem. Ref. Data* **5** 581
[15] Low W and Lawellyn P M 1958 *Phys. Rev.* **110** 382
[16] Seitchik J A, Gossard A C and Jaccarino V 1964 *Phys. Rev.* A **136** 1119
[17] Nelson C V, Boyd G E and Smith W T 1954 *J. Am. Chem. Soc.* **76** 348
[18] De Wette F W 1961 *Phys. Rev.* **123** 103
[19] Tarasov V P, Petrushin S A, Privalov V I, Guerman K E, Kruchkov S V and Buslaev Yu A 1986 *Sov. Koord. Chim. (Engl. Transl.)* **12**, 713
[20] Barnes R G, Borsa F, Segel S L and Torgenson D R 1965 *Phys. Rev.* A **137** 1848
[21] Bastow T J 1997 *Abstracts of XIV International Symposium on Nuclear Quadrupole Interactions*, Pisa, Italia, p 51
[22] Burgstaller A, Ebert H and Voitlärnder J 1986 *Hyperfine Interactions* **89** 1015
[23] Semin G K, Babushkina T A and Jakobson G G 1972 *Application of NQR in Chemistry* (Leningrad: Chemia)
[24] Abart J, Palangie E, Socher W and Voitländer J 1983 *J. Chem. Phys.* **79** 5468
[25] Fuller G H 1976 *J. Phys. Chem. Ref. Data* **5** 835
[26] Das T P and Schmidt P C 1986 *Z. Naturforsch.* **41a** 47